Measurements of Chemical Potentials in Pb-Pb Collisions at $\sqrt{s_{\mathrm{NN}}} = 5.02$ TeV

S. Acharya *et al.*[*]
(ALICE Collaboration)

(Received 13 January 2024; revised 26 March 2024; accepted 3 May 2024; published 26 August 2024)

This Letter presents the most precise measurement to date of the matter-antimatter imbalance at midrapidity in Pb-Pb collisions at a center-of-mass energy per nucleon pair $\sqrt{s_{\mathrm{NN}}} = 5.02$ TeV. Using the Statistical Hadronization framework, it is possible to obtain the value of the electric charge and baryon chemical potentials, $\mu_Q = -0.18 \pm 0.90$ MeV and $\mu_B = 0.71 \pm 0.45$ MeV, with unprecedented precision. A centrality-differential study of the antiparticle-to-particle yield ratios of charged pions, protons, Ω baryons, and light (hyper)nuclei is performed. These results indicate that the system created in Pb-Pb collisions at the LHC is on average baryon-free and electrically neutral at midrapidity.

DOI: 10.1103/PhysRevLett.133.092301

Introduction.—Nuclear matter at extremely high energy densities can be generated in the laboratory through relativistic heavy-ion collisions [1–3]. At the LHC, the beam remnants from the collision are located at rapidities $y \approx \pm 6$ and a fraction of the collision energy is deposited at midrapidity [4]. In this region, particles are formed from a nearly baryon number and electric charge free medium. This process can be described in the color glass condensate model via gluon radiation by static quarks, frozen by time dilation [5]. Conversely, string-fragmentation models explain it through the breaking of color flux tubes. Part of the initial baryon number can be transported to midrapidity via either baryon junction formation [6] or diquark breaking [7]. This phenomenon, known as nuclear stopping, influences the net-baryon density of the system formed at midrapidity [8–10]. The baryon number transport is minimal at the LHC, and the nuclear transparency regime [11] is reached. In this regime, conditions akin to those of the early Universe are replicated, where nearly equal abundances of matter and antimatter were present, as described by the standard cosmological model [12]. Experimentally, one can gauge the extent to which heavy-ion collisions approach the early Universe conditions by measuring the antimatter-to-matter yield ratios across various hadron species.

A comprehensive framework for interpreting these ratios is provided by the Statistical Hadronization Model (SHM) [13–18]. Among the several models that can be used to describe a heavy-ion collision, the SHM is the most successful in describing the yields of all light-flavor hadronic species, which are determined starting from the partition function of the fireball at the freeze-out of inelastic scatterings. This fireball is an equilibrated gas composed of hadrons and resonances. Because of the substantial particle multiplicity and the finite kinematical acceptance, a grand canonical (GC) ensemble description is employed for heavy-ion collisions. In this approach, the conservation of charges, namely the baryon number (B), the electric charge (Q), and strangeness (S), is regulated by the corresponding chemical potentials μ_B, μ_Q, and μ_S, respectively [19,20]. The baryon chemical potential μ_B represents the net-baryon density of the system, with $\mu_B = 0$ corresponding to an equilibrated gas composed of hadrons and resonances with same amount of baryons and antibaryons. The electric charge potential μ_Q encodes the positive-negative charge imbalance of the gas; it is connected to μ_B by the atomic-to-mass-number ratio Z/A of the colliding ions [21,22]. The requirement of strangeness neutrality constrains μ_S throughout the entire volume of the fireball [21,22]. Chemical potentials determine the abundance of hadrons through the fugacity, $\lambda_i = \exp[(B_i\mu_B + Q_i\mu_Q + S_i\mu_S)/T_{\mathrm{ch}}]$, where B_i, Q_i, and S_i denote the quantum numbers of the considered species i, and T_{ch} is the chemical freeze-out temperature, at which hadron yields are determined.

Over the last three decades, the asymmetry between antimatter and matter of the fireball has been systematically studied at different experimental facilities [23–38]. The decreasing trend of μ_B, from about 400 MeV at the SPS to 20 MeV at the top RHIC energy of 200 GeV, and $\mu_B = 0.7 \pm 3.8$ MeV at the LHC is consistent with the decrease of baryon number transport to midrapidity with increasing beam rapidity [36,37,39–79]. The formation of baryon number free matter at midrapidity was first reported in pp collisions by ALICE, which observed that the $\bar{\mathrm{p}}/\mathrm{p}$

[*]Full author list given at the end of the Letter.

yield ratio is compatible with unity [80]. At fixed collision energy, it is also possible to explore nuclear transparency as a function of centrality, i.e., the transverse displacement between the centers of the colliding nuclei, as it affects the dynamics of the colliding nucleons. In particular, a slight increase in μ_B from peripheral to central (head-on) collisions was observed at low energies by STAR at the RHIC beam energy scan [79]. These results were obtained by either comparing the SHM predictions with the measured yields of hadrons and their antimatter counterparts [81] or by directly fitting antiparticle-to-particle yield ratios [76,79].

In this Letter, we report the most precise estimation to date of μ_B and μ_Q obtained from a set of antiparticle-to-particle yield ratios. Compared to previous estimations, the precision of the current results has improved by about an order of magnitude. This improvement in precision is attributed to the proper treatment of the cancelation of particle-antiparticle correlated uncertainties and the reduced dependence on model parameters, such as the system volume, V, which is eliminated in the antiparticle-to-particle yield ratios. The analyzed species are charged pions, protons, Ω^- baryons, and light (hyper)nuclei. (Anti)protons are the most abundantly produced (anti) baryons at midrapidity ($\approx$35 and $\approx$2 protons on average in central and peripheral Pb-Pb collisions, respectively [83]). Consequently, the antiproton-to-proton yield ratio can probe the antibaryon-to-baryon imbalance [80,84] with high precision. On the other hand, the sensitivity to baryon asymmetry is enhanced when light (hyper)nuclei are included because of their larger baryon content. In this work, ^{3}He, its isobar ^{3}H, and hypertriton $^3_\Lambda$H, which is a bound state of a proton, a neutron, and a Λ, along with their antimatter counterparts, are considered. [(Anti)deuterons, d($\bar{\text{d}}$) are not considered in this Letter since the efficiency correction for $\bar{\text{d}}$ is based on the $\bar{\text{d}}$ absorption cross section extracted by the ALICE Collaboration from the measured $\bar{\text{d}}$/d yield ratio itself [85]]. The ratio of oppositely charged pions provides a precise constraint on the imbalance of electric charge, as the yield ratio depends predominantly on μ_Q. Finally, the dependence of antimatter-to-matter ratios on strangeness is probed with (anti)Ω^- baryons, which, unlike (anti)Λ and (anti)Ξ^-, have negligible contamination coming from heavier hadron decays.

The ALICE detector and data analysis.—The results reported in this analysis are obtained from a sample of Pb-Pb collisions at $\sqrt{s_{\rm NN}} = 5.02$ TeV collected in 2018 by ALICE at the LHC. The ALICE apparatus and its performance are described in detail in Refs. [86,87]. The minimum-bias collision and centrality triggers are provided by the V0 system [88], which is composed of two arrays of plastic scintillators covering the forward ($2.8 < \eta < 5.1$) and backward ($-3.7 < \eta < -1.7$) regions of pseudorapidity. The coincidence of signals in both detectors determines the minimum bias trigger. The amplitude of the V0 signal is proportional to the charge deposited in the detectors, which is related to the produced charged-particle multiplicity that, in turn, is controlled by the collision centrality. The V0 amplitude is then used to trigger specific categories of central and semicentral events, and to estimate centrality [89]. Five centrality intervals are considered in this Letter, namely 0%–5%, 5%–10%, 10%–30%, 30%–50%, and 50%–90%, expressed as percentiles of the total hadronic cross section for Pb-Pb collisions. The position of the primary interaction vertex is required to be within a 10 cm wide region centered at the nominal interaction point to profit from the full acceptance of the ALICE central barrel detectors. Events with multiple interaction vertices are rejected to ensure the correct association of reconstructed tracks and primary vertices. The number of events passing these selections is approximately 300×10^6.

Charged pions, protons, ^{3}He, and tritons produced at midrapidity, $|y| < 0.5$, are tracked in the ALICE central barrel: hereafter, charge conjugates are implied unless stated otherwise. The tracks are reconstructed within $|\eta| < 0.8$ and in the full azimuth using the Inner Tracking System (ITS) [90] and the Time Projection Chamber (TPC) [91]. These detectors are placed in a solenoid that provides a uniform magnetic field of 0.5 T parallel to the beam axis. The antiparticle-to-particle yield ratios are measured as a function of the transverse momentum $p_{\rm T}$ in the ranges $0.7 \le p_{\rm T} < 1.6$ GeV/c for π^-/π^+, $0.5 \le p_{\rm T} < 3$ GeV/c for $\bar{\text{p}}$/p, $1.6 \le p_{\rm T} < 3$ GeV/c for $^3\bar{\text{H}}/^3$H, and $2 \le p_{\rm T} < 8$ GeV/c for $^3\overline{\text{He}}/^3$He to select the bulk of the production and ensure good identification performance.

The analysis procedure for extracting particle yields is similar to the one adopted in previous analyses [83,92,93]. Standard selections on the χ^2 of the track fit, on the number of reconstructed track points in the ITS and the TPC, and on the distance of closest approach of the extrapolation of the track to the primary interaction vertex ensure a good reconstruction of tracks originating from the collisions. Particle identification is performed on a statistical basis by measuring the specific energy loss (dE/dx) in both the TPC and the ITS, and particle velocity depending on the transverse momentum of the measured particles with the time-of-flight detector. Further details about the particle identification are provided in the Supplemental Material [94].

The residual contamination due to hyperon weak decays and spallation reactions of primary particles in the apparatus is evaluated by fitting the measured distance of closest approach distribution in the plane transverse to the beam axis with templates computed via Monte Carlo (MC) simulations for the various processes involved [83,92,93]. The extracted yields are corrected for the detector acceptance and candidate selection efficiency, computed using MC simulations, as the fraction of particles reconstructed out of all MC-generated primary particles.

The Pb-Pb event is generated with HIJING [96], while the particles are transported through a realistic model of the ALICE apparatus with GEANT4 [97]. To increase the simulated sample size protons, ^{3}He nuclei, and tritons are injected on top of each HIJING event. The available measurements of hadron inelastic cross sections are used to correct the GEANT4 parametrizations of the corresponding reactions [98–112].

The $^3_\Lambda$H candidates are reconstructed from their two-body charged mesonic decay $^3_\Lambda\mathrm{H} \to {}^3\mathrm{He} + \pi^-$. The reconstruction algorithm is the same as the one applied in previous measurements [113–116]. The Ω^- is reconstructed with a similar procedure from the decay into a charged kaon and a Λ baryon, that, in turn, is reconstructed from its charged two-body decay, $\Omega^- \to \mathrm{K}^- + \Lambda(\to \pi^- + \mathrm{p})$ [117–119]. The ratios are extracted in intervals of proper decay length $ct = cML/p$, with M, L, and p being the mass, trajectory length, and candidate momentum, respectively. In particular, $2 \leq ct < 35$ cm for $^3_\Lambda$H and $1 \leq ct < 10$ cm for Ω^- are used. The $^3_\Lambda$H and Ω^- candidates are selected with boosted decision tree algorithms [120], which are applied on top of preliminary kinematic and topological selections to enhance the background rejection. The boosted decision tree internal parameters and selections are optimized using samples of correctly classified signal and background candidates, as explained in detail in the Supplemental Material [94].

The invariant mass distribution of the selected candidates is fitted with a probability density function built with a kernel density estimation [121,122] in the MC for $^3_\Lambda$H, whereas an extended crystal-ball function is used for the Ω^- signal [123]. An exponential function is used to model the residual background in both cases. The yields extracted as the integral of the signal functions obtained from the fits are corrected by the overall selection efficiency and acceptance computed in the MC simulations. As in previous $^3_\Lambda$H analyses [116], an absorption correction factor is included to account for undetected candidates absorbed in the detector material before their decay.

The following systematic uncertainty contributions are estimated for the antiparticle-to-particle yield ratios: candidate selection and signal extraction, MC data sample size, material budget uncertainty, absorption cross section uncertainties, and magnetic field polarity. The details about the estimation and values of such contributions are reported in the Supplemental Material [94].

Results.—The fully corrected antiparticle-to-particle yield ratios do not exhibit any significant dependence on p_T and ct (see the Supplemental Material [94]). This observation, which is consistent across particle species and centrality intervals, implies that the production spectra of charge-conjugate species only differ by normalization factors proportional to their yields. The antiparticle-to-particle yield ratios of each species are obtained as the averages weighted with the total uncorrelated uncertainties of the p_T- and ct-differential ratios in each centrality interval. For $^3_\Lambda$H, no statistically significant signal is observed in the 50%–90% centrality range.

The chemical potentials μ_B and μ_Q are extracted by fitting the antiparticle-to-particle yield ratios with the predictions of the GC statistical hadronization model using the Thermal-FIST code [22]. The measured ratios and the SHM fit results are reported in Fig. 1. The chemical freeze-out temperature is set to $T_\mathrm{ch} = 155 \pm 2$ MeV, as obtained from a fit to the ALICE data [124,125]: its value is compatible with the pseudocritical temperature extracted with lattice QCD calculations [126]. This value is fixed for all centralities, since in heavy-ion collisions only a mild dependence of T_ch on centrality is observed (less than 3% [35,79,124,127]); additionally, antiparticle-to-particle yield ratios show a negligible dependence on T_ch for $\mu_B \approx 1$ MeV [81]. The uncertainty on T_ch, which is compatible with the range of variations of T_ch observed as a function of centrality, is considered as a centrality-correlated source of systematic uncertainty. The strangeness chemical potential μ_S is constrained in the fit from strangeness conservation. The contribution of strongly decaying resonances is accounted in the model predictions as it cannot be directly disentangled in the data. For the χ^2 minimization, the quadratic sum of statistical and uncorrelated systematic uncertainty is considered. The effect of the centrality-correlated sources is evaluated by repeating the fit to ratios coherently increased or decreased by their uncertainties. The uncertainty assigned to μ_B and μ_Q is half of the difference between the results obtained in the two cases.

In this Letter, yield ratios are analyzed within the GC statistical model also in the most peripheral events, where canonical ensemble formulation is needed for an accurate description of hadron yields by requiring exact conservation of charges over a finite volume [128,129]. It is known, however, that effects connected to the canonical conservation of charges cancel out when considering antiparticle-to-particle yield ratios, and their values are well described by the GC ensemble [15,130]. Indeed, good fit quality is obtained across the 0%–90% centrality range using the GC model to quantify these ratios. In addition, the yield ratio $\bar{\Omega}^+/\Omega^-$ is compatible with unity as expected in the SHM, where it is weakly dependent of μ_B and μ_S for $\mu_B \sim 0$ [16].

The chemical potentials obtained in different centrality intervals are shown in the left panel of Fig. 2. The contours show a negative correlation between μ_B and μ_Q, which is connected to the approximate exponential dependence of antiparticle-to-particle yield ratios on the linear combination of the chemical potentials. The centrality dependence of μ_B and μ_Q is studied by fitting independently the centrality-differential μ_B and μ_Q results with a constant function, taking into account the full correlation matrix of the measurements. Both the correlation matrices and the χ^2 profiles of the fits are reported in the Supplemental

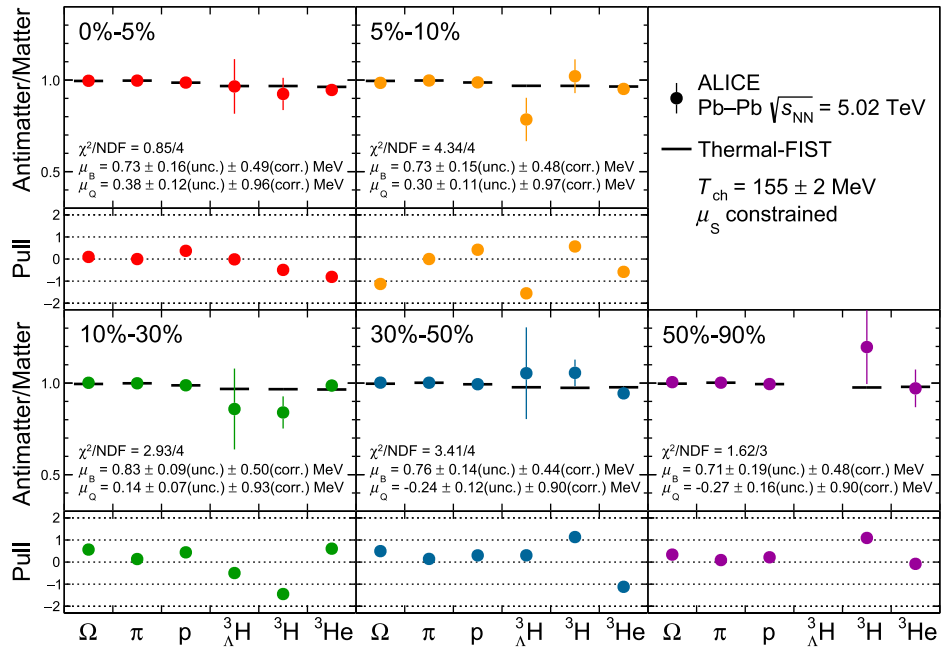

FIG. 1. Upper panels: SHM fits to the measured antiparticle-to-particle yield ratios in different centrality intervals. Error bars show the sum in quadrature of statistical and centrality-uncorrelated systematic uncertainties. When not visible, error bars are hidden by the marker. Lower panels: pull distribution, defined as the difference between data and fit values, normalized to the uncertainty in the data.

Material [94]. The fit probability is $P = 0.97$ for μ_B and $P = 0.64$ for μ_Q: therefore, no evidence of centrality dependence is found, even if a larger μ_B would be expected in more central collisions due to a potentially larger baryon stopping [4]. The fit of the centrality-differential values yields chemical potentials $\mu_B = 0.71 \pm 0.45$ MeV and $\mu_Q = -0.18 \pm 0.90$ MeV, which are compatible with zero within 1.6σ and 0.2σ, respectively. The comparison with the previous data point of μ_B at the LHC [35–38] shows a significant improvement in the precision by a factor larger than 8 (no direct value of μ_Q was provided in that study, see below). These results imply that the system created at midrapidity in Pb-Pb collisions is baryon and electrically neutral on average.

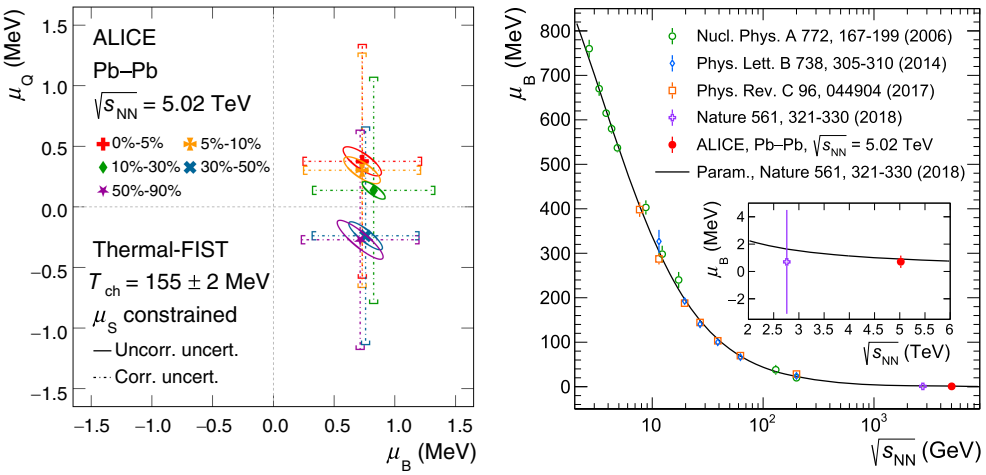

FIG. 2. Left panel: μ_B and μ_Q obtained with Thermal-FIST [22] in different centrality intervals. The centrality-correlated and centrality-uncorrelated uncertainties are represented with error bars and ellipses, respectively. Right panel: μ_B extracted from data collected in Au-Au and Pb-Pb collisions at the AGS (E802, E866, E877, E895, E896, E917 Collaborations), SPS (NA44, NA49, NA47 Collaborations), RHIC (BRAHMS, PHENIX, STAR Collaboration), and LHC (ALICE Collaboration) as a function of the center-of-mass energy per nucleon-nucleon pair [76,78,79], and phenomenological parametrization of $\mu_B(\sqrt{s_{NN}})$ [36]. The inset shows more in detail the results obtained at the LHC [36].

As a consequence, this observation shows that the nuclear transparency regime is reached, i.e., baryon transport from the colliding ions to the interaction region is negligible. Because of the absence of any centrality dependence, it is also concluded that nuclear transparency is achieved even in central Pb-Pb collisions, where a larger-than-zero μ_B could be expected from a more significant baryon number transport at midrapidity.

As a cross check, the SHM fits described above are repeated by also constraining μ_Q from initial conditions via conservation laws, as it was done also in past measurements [36,76,79]. Specifically, the μ_Q/μ_B ratio is fixed by requiring that the average charge-to-baryon density ratio of the created hadron system, $\langle n_Q\rangle/\langle n_B\rangle$, is equivalent to the Z/A ratio of colliding nuclei, i.e., $\langle n_Q\rangle/\langle n_B\rangle = Z/A \approx 0.4$ for ^{208}Pb [21]. The μ_B values extracted from the fits in each centrality interval are successfully fitted with a constant function (fit probability $P = 0.09$). The resulting μ_B value is compatible with the one reported above within uncertainties. Similar results are obtained by fitting the antiparticle-to-particle yield ratios using the GSI-Heidelberg model [15,37,76], with $T_{\rm ch} = 156.6 \pm 1.7$ MeV [38] and μ_Q is fixed to initial conditions: the average value across centrality is $\mu_B = 0.90 \pm 0.43$ MeV. The χ^2 profile of the fit is reported in the Supplemental Material [94]. Using the values of μ_B and μ_Q extracted in the 5% most central collisions, the inclusive net-proton density at midrapidity, $2/\langle N_{\rm part}\rangle {\rm d}N_{\rm p-\bar{p}}/{\rm d}y$, can be computed in the SHM framework. The value extracted with Thermal-FIST is $(3.4 \pm 1.4) \times 10^{-3}$, while using the GSI-Heidelberg model, a value of $5.9^{+2.2}_{-2.8} \times 10^{-3}$ is obtained. In both cases, the obtained results agree with the exponential trend as a function of beam rapidity predicted by the baryon-junction mechanism [131].

The right panel of Fig. 2 shows the comparison of the current with past estimations of μ_B as a function of the center-of-mass energy of the collision [36,76,78,79]. The comparison with the previous LHC data point is highlighted in the inset of the figure. The result reported in this Letter is compatible with the extrapolation of the phenomenological parametrization based on previous data and reported in Ref. [36].

Conclusions.—In summary, the most precise measurement of the asymmetry between matter and antimatter at the LHC is reported in this Letter. The asymmetry is quantified through antiparticle-to-particle yield ratios of different hadrons, which are analyzed within the Statistical Hadronization framework to extract the chemical potentials μ_B and μ_Q. The GC version of the model accurately describes the antiparticle-to-particle yield ratios across centrality, indicating the elimination of effects from canonical charge conservation in peripheral events. The cancelation of correlated uncertainties in these ratios leads to a significant improvement in the μ_B precision: the uncertainty on the obtained value is about 1 order of magnitude smaller than the previously published one [36]. In addition, a direct estimation of μ_Q is provided. Furthermore, the first centrality-differential study of chemical potentials at the LHC is reported in this Letter. The obtained chemical potentials are consistent with zero, i.e., with the nuclear transparency regime being reached across the full centrality range, thus indicating that baryon transport to midrapidity is negligible even in the most central events at the LHC.

The ALICE Collaboration would like to thank all its engineers and technicians for their invaluable contributions to the construction of the experiment and the CERN accelerator teams for the outstanding performance of the LHC complex. The ALICE Collaboration gratefully acknowledges the resources and support provided by all Grid centers and the Worldwide LHC Computing Grid (WLCG) Collaboration. The ALICE Collaboration acknowledges the following funding agencies for their support in building and running the ALICE detector: A. I. Alikhanyan National Science Laboratory (Yerevan Physics Institute) Foundation (ANSL), State Committee of Science and World Federation of Scientists (WFS), Armenia; Austrian Academy of Sciences, Austrian Science Fund (FWF): [M 2467-N36] and Nationalstiftung für Forschung, Technologie und Entwicklung, Austria; Ministry of Communications and High Technologies, National Nuclear Research Center, Azerbaijan; Conselho Nacional de Desenvolvimento Científico e Tecnológico (CNPq), Financiadora de Estudos e Projetos (Finep), Fundação de Amparo à Pesquisa do Estado de São Paulo (FAPESP), and Universidade Federal do Rio Grande do Sul (UFRGS), Brazil; Bulgarian Ministry of Education and Science, within the National Roadmap for Research Infrastructures 2020-2027 (object CERN), Bulgaria; Ministry of Education of China (MOEC), Ministry of Science & Technology of China (MSTC), and National Natural Science Foundation of China (NSFC), China; Ministry of Science and Education and Croatian Science Foundation, Croatia; Centro de Aplicaciones Tecnológicas y Desarrollo Nuclear (CEADEN), Cubaenergía, Cuba; Ministry of Education, Youth and Sports of the Czech Republic, Czech Republic; The Danish Council for Independent Research | Natural Sciences, the VILLUM FONDEN and Danish National Research Foundation (DNRF), Denmark; Helsinki Institute of Physics (HIP), Finland; Commissariat à l'Energie Atomique (CEA) and Institut National de Physique Nucléaire et de Physique des Particules (IN2P3), and Centre National de la Recherche Scientifique (CNRS), France; Bundesministerium für Bildung und Forschung (BMBF) and GSI Helmholtzzentrum für Schwerionenforschung GmbH, Germany; General Secretariat for Research and Technology, Ministry of Education, Research and Religions, Greece; National Research, Development and Innovation Office, Hungary; Department of Atomic Energy

Government of India (DAE), Department of Science and Technology, Government of India (DST), University Grants Commission, Government of India (UGC), and Council of Scientific and Industrial Research (CSIR), India; National Research and Innovation Agency—BRIN, Indonesia; Istituto Nazionale di Fisica Nucleare (INFN), Italy; Japanese Ministry of Education, Culture, Sports, Science and Technology (MEXT) and Japan Society for the Promotion of Science (JSPS) KAKENHI, Japan; Consejo Nacional de Ciencia (CONACYT) y Tecnología, through Fondo de Cooperación Internacional en Ciencia y Tecnología (FONCICYT), and Dirección General de Asuntos del Personal Academico (DGAPA), Mexico; Nederlandse Organisatie voor Wetenschappelijk Onderzoek (NWO), Netherlands; The Research Council of Norway, Norway; Commission on Science and Technology for Sustainable Development in the South (COMSATS), Pakistan; Pontificia Universidad Católica del Perú, Peru; Ministry of Education and Science, National Science Centre and WUT ID-UB, Poland; Korea Institute of Science and Technology Information and National Research Foundation of Korea (NRF), Republic of Korea; Ministry of Education and Scientific Research, Institute of Atomic Physics, Ministry of Research and Innovation and Institute of Atomic Physics and Universitatea Nationala de Stiinta si Tehnologie Politehnica Bucuresti, Romania; Ministry of Education, Science, Research and Sport of the Slovak Republic, Slovakia; National Research Foundation of South Africa, South Africa; Swedish Research Council (VR) and Knut & Alice Wallenberg Foundation (KAW), Sweden; European Organization for Nuclear Research, Switzerland; Suranaree University of Technology (SUT), National Science and Technology Development Agency (NSTDA), and National Science, Research and Innovation Fund (NSRF via PMU-B B05F650021), Thailand; Turkish Energy, Nuclear and Mineral Research Agency (TENMAK), Turkey; National Academy of Sciences of Ukraine, Ukraine; Science and Technology Facilities Council (STFC), United Kingdom; National Science Foundation of the United States of America (NSF) and United States Department of Energy, Office of Nuclear Physics (DOE NP), USA. In addition, individual groups or members have received support from Czech Science Foundation (Grant No. 23-07499S), Czech Republic; European Research Council, Strong 2020—Horizon 2020 (Grants No. 950692, No. 824093), European Union; ICSC—Centro Nazionale di Ricerca in High Performance Computing, Big Data and Quantum Computing, European Union—NextGenerationEU; Academy of Finland (Center of Excellence in Quark Matter) (Grants No. 346327, No. 346328), Finland.

[1] E. Shuryak, Strongly coupled quark-gluon plasma in heavy ion collisions, Rev. Mod. Phys. **89**, 035001 (2017).

[2] P. Braun-Munzinger, V. Koch, T. Schäfer, and J. Stachel, Properties of hot and dense matter from relativistic heavy ion collisions, Phys. Rep. **621**, 76 (2016).

[3] W. Busza, K. Rajagopal, and W. van der Schee, Heavy ion collisions: The big picture, and the big questions, Annu. Rev. Nucl. Part. Sci. **68**, 339 (2018).

[4] Y. Mehtar-Tani and G. Wolschin, Baryon stopping and saturation physics in relativistic collisions, Phys. Rev. C **80**, 054905 (2009).

[5] L. D. McLerran and R. Venugopalan, Computing quark and gluon distribution functions for very large nuclei, Phys. Rev. D **49**, 2233 (1994).

[6] S. E. Vance, M. Gyulassy, and X. N. Wang, Baryon junction stopping at the SPS and RHIC via HIJING/B, Nucl. Phys. **A638**, 395C (1998).

[7] A. Capella and B. Z. Kopeliovich, Novel mechanism of nucleon stopping in heavy ion collisions, Phys. Lett. B **381**, 325 (1996).

[8] F. Videbaek, Stopping and baryon transport in heavy ion reactions, J. Phys. Conf. Ser. **50**, 134 (2006).

[9] V. Topor Pop, J. Barrette, C. Gale, S. Jeon, and M. Gyulassy, Stopping power from SPS to LHC energies, J. Phys. G **35**, 054001 (2008).

[10] J. Hoelck and G. Wolschin, Baryon stopping as a relativistic Markov process in phase space, Phys. Rev. Res. **2**, 033409 (2020).

[11] H. Elfner and B. Müller, The exploration of hot and dense nuclear matter: Introduction to relativistic heavy-ion physics, J. Phys. G **50**, 103001 (2023).

[12] M. J. Fromerth, I. Kuznetsova, L. Labun, J. Letessier, and J. Rafelski, From quark-gluon universe to neutrino decoupling: $200 < T < 2$ MeV, Acta Phys. Pol. B **43**, 2261 (2012).

[13] P. Braun-Munzinger and J. Stachel, Dynamics of ultra-relativistic nuclear collisions with heavy beams: An experimental overview, Nucl. Phys. **A638**, 3 (1998).

[14] J. Cleymans and K. Redlich, Unified description of freezeout parameters in relativistic heavy ion collisions, Phys. Rev. Lett. **81**, 5284 (1998).

[15] P. Braun-Munzinger, K. Redlich, and J. Stachel, Particle production in heavy ion collisions, in *Quark–Gluon Plasma 3* (World Scientific, Singapore, 2004), pp. 491–599, 10.1142/5029.

[16] J. Cleymans, H. Oeschler, K. Redlich, and S. Wheaton, Comparison of chemical freeze-out criteria in heavy-ion collisions, Phys. Rev. C **73**, 034905 (2006).

[17] P. Braun-Munzinger and J. Wambach, The phase diagram of strongly-interacting matter, Rev. Mod. Phys. **81**, 1031 (2009).

[18] V. Vovchenko and H. Stoecker, Examination of the sensitivity of the thermal fits to heavy-ion hadron yield data to the modeling of the eigenvolume interactions, Phys. Rev. C **95**, 044904 (2017).

[19] R. Hagedorn and K. Redlich, Statistical thermodynamics in relativistic particle and ion physics: Canonical or grand canonical?, Z. Phys. C **27**, 541 (1985).

[20] K. Redlich, J. Cleymans, H. Oeschler, and A. Tounsi, Conservation laws and particle production in heavy ion collisions, AIP Conf. Proc. **594**, 318 (2002).

[21] A. Bazavov *et al.*, Freeze-out conditions in heavy ion collisions from QCD thermodynamics, Phys. Rev. Lett. **109**, 192302 (2012).

[22] V. Vovchenko and H. Stoecker, Thermal-FIST: A package for heavy-ion collisions and hadronic equation of state, Comput. Phys. Commun. **244**, 295 (2019).

[23] J. Stachel and P. Braun-Munzinger, Stopping in high-energy nucleus nucleus collisions: Analysis in the Landau hydrodynamic model, Phys. Lett. B **216**, 1 (1989).

[24] P. Braun-Munzinger, J. Stachel, J. P. Wessels, and N. Xu, Thermal equilibration and expansion in nucleus-nucleus collisions at the AGS, Phys. Lett. B **344**, 43 (1995).

[25] L. Ahle *et al.* (E802 Collaboration), Anti-proton production in Au + Au collisions at 11.7 AGeV/c, Phys. Rev. Lett. **81**, 2650 (1998).

[26] F. Siklér *et al.* (NA49 Collaboration), Hadron production in nuclear collisions from the NA49 experiment at 158 GeV/c · A, Nucl. Phys. **A661**, 45 (1999).

[27] P. Braun-Munzinger, I. Heppe, and J. Stachel, Chemical equilibration in Pb + Pb collisions at the SPS, Phys. Lett. B **465**, 15 (1999).

[28] F. Becattini, J. Cleymans, A. Keranen, E. Suhonen, and K. Redlich, Features of particle multiplicities and strangeness production in central heavy ion collisions between 1.7 AGeV/c and 158 AGeV/c, Phys. Rev. C **64**, 024901 (2001).

[29] P. Braun-Munzinger and J. Stachel, Particle ratios, equilibration, and the QCD phase boundary, J. Phys. G **28**, 1971 (2002).

[30] C. Adler *et al.* (STAR Collaboration), Midrapidity anti-proton to proton ratio from Au + Au collisions at $\sqrt{s_{\mathrm{NN}}} = 130$ GeV, Phys. Rev. Lett. **86**, 4778 (2001); **90**, 119903(E) (2003).

[31] I. G. Bearden *et al.* (BRAHMS Collaboration), Rapidity dependence of anti-proton to proton ratios in Au + A collisions at $\sqrt{s_{\mathrm{NN}}} = 130$ GeV, Phys. Rev. Lett. **87**, 112305 (2001).

[32] P. Braun-Munzinger, D. Magestro, K. Redlich, and J. Stachel, Hadron production in Au-Au collisions at RHIC, Phys. Lett. B **518**, 41 (2001).

[33] D. Magestro, Evidence for chemical equilibration at RHIC, J. Phys. G **28**, 1745 (2002).

[34] F. Becattini, M. Gazdzicki, A. Keranen, J. Manninen, and R. Stock, Chemical equilibrium study in nucleus nucleus collisions at relativistic energies, Phys. Rev. C **69**, 024905 (2004).

[35] B. Abelev *et al.* (ALICE Collaboration), Centrality dependence of π, K, p production in Pb-Pb collisions at $\sqrt{s_{\mathrm{NN}}} = 2.76$ TeV, Phys. Rev. C **88**, 044910 (2013).

[36] A. Andronic, P. Braun-Munzinger, K. Redlich, and J. Stachel, Decoding the phase structure of QCD via particle production at high energy, Nature (London) **561**, 321 (2018).

[37] A. Andronic, P. Braun-Munzinger, B. Friman, P. M. Lo, K. Redlich, and J. Stachel, The thermal proton yield anomaly in Pb-Pb collisions at the LHC and its resolution, Phys. Lett. B **792**, 304 (2019).

[38] A. Andronic, P. Braun-Munzinger, K. Redlich, and J. Stachel, Hadron yields in central nucleus-nucleus collisions, the statistical hadronization model and the QCD phase diagram, Acta Phys. Pol. B Proc. Suppl. **14**, 341 (2021).

[39] H. Appelshäuser *et al.* (NA49 Collaboration), Ξ and $\bar{\Xi}$ production in 158-GeV/nucleon Pb + Pb collisions, Phys. Lett. B **444**, 523 (1998).

[40] L. Ahle *et al.* (E802 Collaboration), Kaon production in Au + Au collisions at 11.6*A* GeV/*c*, Phys. Rev. C **58**, 3523 (1998).

[41] L. Ahle *et al.* (E802 Collaboration), Proton and deuteron production in Au + Au reactions at 11.6/A-GeV/c, Phys. Rev. C **60**, 064901 (1999).

[42] L. Ahle *et al.* (E866, E917 Collaboration), Excitation function of K^+ and π^+ production in Au + Au reactions at 2-10 A GeV, Phys. Lett. B **476**, 1 (2000).

[43] J. Barrette *et al.* (E877 Collaboration), Proton and pion production in Au + Au collisions at 10.8A-GeV/c, Phys. Rev. C **62**, 024901 (2000).

[44] S. Afanasiev *et al.*, Production of ϕ-mesons in p + p, p + pb and central pb + pb collisions at $E_{\mathrm{beam}} = 158$ A GeV, Phys. Lett. B **491**, 59 (2000).

[45] L. Ahle *et al.* (E866, E917 Collaboration), An excitation function of K^- and K^+ production in Au + Au reactions at the AGS, Phys. Lett. B **490**, 53 (2000).

[46] B. B. Back *et al.* (E917 Collaboration), Baryon rapidity loss in relativistic Au + Au collisions, Phys. Rev. Lett. **86**, 1970 (2001).

[47] C. Pinkenburg *et al.* (E895 Collaboration), Production and collective behavior of strange particles in Au + Au collisions at 2-8 A GeV, Nucl. Phys. **A698**, 495 (2002).

[48] J. L. Klay *et al.* (E895 Collaboration), Longitudinal flow from (2-8) A GeV Au + Au collisions at the Brookhaven AGS, Phys. Rev. Lett. **88**, 102301 (2002).

[49] S. Albergo *et al.*, Λ spectra in 11.6 *A*GeV/c Au-Au collisions, Phys. Rev. Lett. **88**, 062301 (2002).

[50] C. Adler *et al.* (STAR Collaboration), Kaon production and kaon to pion ratio in Au + Au collisions at $\sqrt{s_{\mathrm{NN}}} = 130$ GeV, Phys. Lett. B **595**, 143 (2004).

[51] C. Adler *et al.* (STAR Collaboration), $K^*(892)^0$ production in relativistic heavy ion collisions at $\sqrt{s_{\mathrm{NN}}} = 130$ GeV, Phys. Rev. C **66**, 061901 (2002).

[52] S. V. Afanasiev *et al.* (NA49 Collaboration), Energy dependence of pion and kaon production in central Pb + Pb collisions, Phys. Rev. C **66**, 054902 (2002).

[53] K. Adcox *et al.* (PHENIX Collaboration), Measurement of the Λ and $\bar{\Lambda}$ particles in Au + Au collisions at $\sqrt{s_{\mathrm{NN}}} = 130$ GeV, Phys. Rev. Lett. **89**, 092302 (2002).

[54] C. Adler *et al.* (STAR Collaboration), Midrapidity ϕ production in Au + Au collisions at $\sqrt{s_{\mathrm{NN}}} = 130$ GeV, Phys. Rev. C **65**, 041901 (2002).

[55] I. G. Bearden *et al.* (NA44 Collaboration), Particle production in central Pb + Pb collisions at 158-A-GeV/c, Phys. Rev. C **66**, 044907 (2002).

[56] B. B. Back *et al.* (E917 Collaboration), Production of ϕ mesons in Au + Au collisions at 11.7-A-GeV/c, Phys. Rev. C **69**, 054901 (2004).

[57] J. L. Klay *et al.* (E895 Collaboration), Charged pion production in 2 to 8A GeV central Au + Au collisions, Phys. Rev. C **68**, 054905 (2003).

[58] P. Chung *et al.* (E895 Collaboration), Near threshold production of the multistrange Ξ^- hyperon, Phys. Rev. Lett. **91**, 202301 (2003).

[59] K. Adcox *et al.* (PHENIX Collaboration), Single identified hadron spectra from $\sqrt{s_{\rm NN}} = 130$ GeV Au + Au collisions, Phys. Rev. C **69**, 024904 (2004).

[60] T. Anticic *et al.* (NA49 Collaboration), Energy and centrality dependence of deuteron and proton production in Pb + Pb collisions at relativistic energies, Phys. Rev. C **69**, 024902 (2004).

[61] T. Anticic *et al.* (NA49 Collaboration), Λ and $\bar{\Lambda}$ production in central Pb-Pb collisions at 40-A-GeV, 80-A-GeV and 158-A-GeV, Phys. Rev. Lett. **93**, 022302 (2004).

[62] S. S. Adler *et al.* (PHENIX Collaboration), Identified charged particle spectra and yields in Au + Au collisions at $\sqrt{s_{\rm NN}} = 200$ GeV, Phys. Rev. C **69**, 034909 (2004).

[63] J. Adams *et al.* (STAR Collaboration), Multistrange baryon production in Au-Au collisions at $\sqrt{s_{\rm NN}} = 130$ GeV, Phys. Rev. Lett. **92**, 182301 (2004).

[64] J. Adams *et al.* (STAR Collaboration), Identified particle distributions in pp and Au + Au collisions at $\sqrt{s_{\rm NN}} =$ 200 GeV, Phys. Rev. Lett. **92**, 112301 (2004).

[65] C. Alt *et al.* (NA49 Collaboration), Ω^- and $\bar{\Omega}^+$ production in central Pb + Pb collisions at 40-AGeV and 158-AGeV, Phys. Rev. Lett. **94**, 192301 (2005).

[66] F. Antinori *et al.* (NA57 Collaboration), Energy dependence of hyperon production in nucleus nucleus collisions at SPS, Phys. Lett. B **595**, 68 (2004).

[67] J. Adams *et al.* (STAR Collaboration), $K(892)^*$ resonance production in Au + Au and p + p collisions at $\sqrt{s_{\rm NN}} =$ 200 GeV at STAR, Phys. Rev. C **71**, 064902 (2005).

[68] S. S. Adler *et al.* (PHENIX Collaboration), Production of ϕ mesons at mid-rapidity in $\sqrt{s_{\rm NN}} = 200$ GeV Au + Au collisions at RHIC, Phys. Rev. C **72**, 014903 (2005).

[69] S. S. Adler *et al.* (PHENIX Collaboration), Deuteron and antideuteron production in Au + Au collisions at $\sqrt{s_{\rm NN}} = 200$ GeV, Phys. Rev. Lett. **94**, 122302 (2005).

[70] J. Adams *et al.* (STAR Collaboration), phi meson production in Au + Au and p + p collisions at $\sqrt{s_{\rm NN}} = 200$ GeV, Phys. Lett. B **612**, 181 (2005).

[71] A. E. M. Billmeier (for the STAR Collaboration), Strange and multi-strange particle ratios in p + p reactions at $\sqrt{s} = 200$ GeV at RHIC, J. Phys. G **30**, S363 (2003).

[72] H.-b. Zhang (STAR Collaboration), Δ, K^* and ρ resonance production and their probing of freezeout dynamics at RHIC, in *Proceedings of the 17th International Conference on Ultra Relativistic Nucleus-Nucleus Collisions (Quark Matter 2004)* (2004); arXiv:nucl-ex/0403010.

[73] O. Y. Barannikova (STAR Collaboration), Probing collision dynamics at RHIC, in *Proceedings of the 17th International Conference on Ultra Relativistic Nucleus-Nucleus Collisions (Quark Matter 2004)* (2004); arXiv:nucl-ex/0403014.

[74] F. Antinori *et al.* (NA57 Collaboration), Rapidity distributions around mid-rapidity of strange particles in Pb-Pb collisions at 158-A-GeV/c, J. Phys. G **31**, 1345 (2005).

[75] I. Arsene *et al.* (BRAHMS Collaboration), Centrality dependent particle production at $y = 0$ and $y \sim 1$ in Au + Au collisions at $\sqrt{s_{\rm NN}} = 200$ GeV, Phys. Rev. C **72**, 014908 (2005).

[76] A. Andronic, P. Braun-Munzinger, and J. Stachel, Hadron production in central nucleus-nucleus collisions at chemical freeze-out, Nucl. Phys. **A772**, 167 (2006).

[77] A. Andronic, P. Braun-Munzinger, and J. Stachel, Thermal hadron production in relativistic nuclear collisions: The Hadron mass spectrum, the horn, and the QCD phase transition, Phys. Lett. B **673**, 142 (2009); **678**, 516(E) (2009).

[78] P. Alba, W. Alberico, R. Bellwied, M. Bluhm, V. Mantovani Sarti, M. Nahrgang, and C. Ratti, Freeze-out conditions from net-proton and net-charge fluctuations at RHIC, Phys. Lett. B **738**, 305 (2014).

[79] L. Adamczyk *et al.* (STAR Collaboration), Bulk properties of the medium produced in relativistic heavy-ion collisions from the beam energy scan program, Phys. Rev. C **96**, 044904 (2017).

[80] K. Aamodt *et al.* (ALICE Collaboration), Midrapidity antiproton-to-proton ratio in pp collisions at $\sqrt{s} = 0.9$ and 7 TeV measured by the ALICE experiment, Phys. Rev. Lett. **105**, 072002 (2010).

[81] J. Cleymans, I. Kraus, H. Oeschler, K. Redlich, and S. Wheaton, Statistical model predictions for particle ratios at $\sqrt{s_{\rm NN}} = 5.5$ TeV, Phys. Rev. C **74**, 034903 (2006).

[82] K. Adcox *et al.* (PHENIX Collaboration), Centrality dependence of $\pi^{+/-}$, $K^{+/-}$, p, and $\bar{p}$ production from $\sqrt{s_{\rm NN}} = 130$ GeV Au + Au collisions at RHIC, Phys. Rev. Lett. **88**, 242301 (2002).

[83] S. Acharya *et al.* (ALICE Collaboration), Production of charged pions, kaons, and (anti-)protons in Pb-Pb and inelastic pp collisions at $\sqrt{s_{\rm NN}} = 5.02$ TeV, Phys. Rev. C **101**, 044907 (2020).

[84] E. Abbas *et al.* (ALICE Collaboration), Mid-rapidity anti-baryon to baryon ratios in pp collisions at $\sqrt{s} = 0.9$, 2.76 and 7 TeV measured by ALICE, Eur. Phys. J. C **73**, 2496 (2013).

[85] S. Acharya *et al.* (ALICE Collaboration), Measurement of the low-energy antideuteron inelastic cross section, Phys. Rev. Lett. **125**, 162001 (2020).

[86] K. Aamodt *et al.* (ALICE Collaboration), The ALICE experiment at the CERN LHC, J. Instrum. **3**, S08002 (2008).

[87] B. B. Abelev *et al.* (ALICE Collaboration), Performance of the ALICE experiment at the CERN LHC, Int. J. Mod. Phys. A **29**, 1430044 (2014).

[88] E. Abbas *et al.* (ALICE Collaboration), Performance of the ALICE VZERO system, J. Instrum. **8**, P10016 (2013).

[89] ALICE Collaboration, Centrality determination in heavy ion collisions, Report No. ALICE-PUBLIC-2018-011, CERN, European Organization for Nuclear Research, 2018, https://cds.cern.ch/record/2636623.

[90] K. Aamodt *et al.* (ALICE Collaboration), Alignment of the ALICE inner tracking system with cosmic-ray tracks, J. Instrum. **5**, P03003 (2010).

[91] J. Alme *et al.*, The ALICE TPC, a large 3-dimensional tracking device with fast readout for ultra-high multiplicity events, Nucl. Instrum. Methods Phys. Res., Sect. A **622**, 316 (2010).

[92] J. Adam *et al.* (ALICE Collaboration), Production of light nuclei and anti-nuclei in pp and Pb-Pb collisions at energies available at the CERN Large Hadron Collider, Phys. Rev. C **93**, 024917 (2016).

[93] S. Acharya *et al.* (ALICE Collaboration), Light (anti)nuclei production in Pb-Pb collisions at $\sqrt{s_{\rm NN}} = 5.02$ TeV, Phys. Rev. C **107**, 064904 (2023).

[94] See Supplemental Material at http://link.aps.org/supplemental/10.1103/PhysRevLett.133.092301, which includes Ref. [95], for additional information about the experimental methods.

[95] E. Schnedermann, J. Sollfrank, and U. W. Heinz, Thermal phenomenology of hadrons from 200A GeV S + S collisions, Phys. Rev. C **48**, 2462 (1993).

[96] X.-N. Wang and M. Gyulassy, HIJING: A Monte Carlo model for multiple jet production in pp, pA and AA collisions, Phys. Rev. D **44**, 3501 (1991).

[97] S. Agostinelli *et al.* (GEANT4 Collaboration), GEANT4–a simulation toolkit, Nucl. Instrum. Methods Phys. Res., Sect. A **506**, 250 (2003).

[98] F. F. Chen, C. P. Leavitt, and A. M. Shapiro, Attenuation cross sections for 860-MeV protons, Phys. Rev. **99**, 857 (1955).

[99] N. E. Booth, B. Ledley, D. Walker, and D. H. White, Nuclear cross sections for 900 MeV protons., Proc. Phys. Soc. (London), Sect. A **70**, 209 (1957).

[100] N. T. Porile, Simple nuclear reactions of indium with 30 and 2.9 GeV protons, Phys. Rev. **128**, 1916 (1962).

[101] O. Artun *et al.*, Multinucleon removal induced by high-energy protons, Phys. Rev. Lett. **35**, 773 (1975).

[102] M. E. Sadler, P. P. Singh, J. Jastrzebski, L. L. Rutledge, Jr., and R. E. Segel, Interaction of 80–164 MeV protons with nickel isotopes, Phys. Rev. C **21**, 2303 (1980).

[103] D. Ashery, I. Navon, G. Azuelos, H. K. Walter, H. J. Pfeiffer, and F. W. Schleputz, True absorption and scattering of pions on nuclei, Phys. Rev. C **23**, 2173 (1981).

[104] K. Nakamura, J. Chiba, T. Fujii, H. Iwasaki, T. Kageyama, S. Kuribayashi, T. Sumiyoshi, T. Takeda, H. Ikeda, and Y. Takada, Absorption and forward scattering of antiprotons by C, Al, and Cu nuclei in the region 470–880 MeV/c, Phys. Rev. Lett. **52**, 731 (1984).

[105] J. A. McGill, G. W. Hoffmann, M. L. Barlett, R. W. Fergerson, E. C. Milner, R. E. Chrien, R. J. Sutter, T. Kozlowski, and R. L. Stearns, Proton + nucleus inclusive (p, p') scattering at 800 MeV, Phys. Rev. C **29**, 204 (1984).

[106] N. G. Zaitseva, E. Rurarz, M. Vobecky, K. H. Hwan, K. Nowak, T. Tethal, V. A. Khalkin, and L. M. Popinenkova, Excitation function and yield for ^{97}Ru production in ^{99}Tc$(p, 3n)^{97}$Ru reaction in 20–100 MeV proton energy range, Radiochim. Acta **56**, 59 (1992).

[107] V. F. Kuzichev, Y. B. Lepikhin, and V. A. Smirnitsky, The anti-proton—nuclei annihilation cross-section at the momentum range from 0.70 GeV/c to 2.5 GeV/c, Nucl. Phys. **A576**, 581 (1994).

[108] C. M. Herbach *et al.*, Systematic investigation of 1.2 GeV proton-induced spallation reactions on targets between Al and U, Nucl. Instrum. Methods Phys. Res., Sect. A **562**, 729 (2006).

[109] M. Zamani, S. Stoulos, M. Fragopoulou, M. Manolopoulou, and M. Krivopustov, Indirect measurement of inelastic cross section of relativistic protons in Pb target, Ann. Nucl. Energy **37**, 923 (2010).

[110] D. W. Bardayan *et al.*, Inelastic ^{17}F$(p, p)^{17}$F scattering at $E_{c.m.} = 3$ MeV and the ^{14}O$(\alpha, p)^{17}$F reaction rate, Phys. Rev. C **81**, 065802 (2010).

[111] S. Acharya *et al.* (ALICE Collaboration), Measurement of anti-^{3}He nuclei absorption in matter and impact on their propagation in the Galaxy, Nat. Phys. **19**, 61 (2023).

[112] S. Acharya *et al.* (ALICE Collaboration), Measurement of the low-energy antitriton inelastic cross section, Phys. Lett. B **848**, 138337 (2024).

[113] J. Adam *et al.* (ALICE Collaboration), $^3_\Lambda$H and $^3_{\bar\Lambda}\bar{\rm H}$ production in Pb-Pb collisions at $\sqrt{s_{\rm NN}} = 2.76$ TeV, Phys. Lett. B **754**, 360 (2016).

[114] S. Acharya *et al.* (ALICE Collaboration), $^3_\Lambda$H and $^3_{\bar\Lambda}\bar{\rm H}$ lifetime measurement in Pb-Pb collisions at $\sqrt{s_{\rm NN}} =$ 5.02 TeV via two-body decay, Phys. Lett. B **797**, 134905 (2019).

[115] S. Acharya *et al.* (ALICE Collaboration), Hypertriton production in p-Pb collisions at $\sqrt{s_{\rm NN}} = 5.02$ TeV, Phys. Rev. Lett. **128**, 252003 (2022).

[116] S. Acharya *et al.* (ALICE Collaboration), Measurement of the lifetime and Λ separation energy of $^3_\Lambda$H, Phys. Rev. Lett. **131**, 102302 (2023).

[117] B. Abelev *et al.* (ALICE Collaboration), Multi-strange baryon production in pp collisions at $\sqrt{s} = 7$ TeV with ALICE, Phys. Lett. B **712**, 309 (2012).

[118] B. B. Abelev *et al.* (ALICE Collaboration), Multi-strange baryon production at mid-rapidity in Pb-Pb collisions at $\sqrt{s_{\rm NN}} = 2.76$ TeV, Phys. Lett. B **728**, 216 (2014); **734**, 409(E) (2014).

[119] J. Adam *et al.* (ALICE Collaboration), Multi-strange baryon production in p-Pb collisions at $\sqrt{s_{\rm NN}} = 5.02$ TeV, Phys. Lett. B **758**, 389 (2016).

[120] T. Chen and C. Guestrin, Xgboost: A scalable tree boosting system, in *Proceedings of the 22nd ACM SIGKDD International Conference on Knowledge Discovery and Data Mining, KDD '16* (Association for Computing Machinery, New York, NY, USA, 2016), pp. 785–794.

[121] K. S. Cranmer, Kernel estimation in high-energy physics, Comput. Phys. Commun. **136**, 198 (2001).

[122] W. Verkerke and D. P. Kirkby, The RooFit toolkit for data modeling, eConf **C0303241**, MOLT007 (2003).

[123] J. Adam *et al.* (ALICE Collaboration), Quarkonium signal extraction in ALICE, CERN, European Organization for Nuclear Research, Report No. ALICE-PUBLIC-2015-006, 2015, https://cds.cern.ch/record/2060096/.

[124] V. Vovchenko, M. I. Gorenstein, and H. Stoecker, Finite resonance widths influence the thermal-model description of hadron yields, Phys. Rev. C **98**, 034906 (2018).

[125] ALICE Collaboration, The ALICE experiment—A journey through QCD, arXiv:2211.04384.

[126] S. Borsanyi, Z. Fodor, J. N. Guenther, R. Kara, S. D. Katz, P. Parotto, A. Pasztor, C. Ratti, and K. K. Szabo, QCD crossover at finite chemical potential from lattice simulations, Phys. Rev. Lett. **125**, 052001 (2020).

[127] B. I. Abelev *et al.* (STAR Collaboration), Systematic measurements of identified particle spectra in pp, d + Au and Au + Au collisions from STAR, Phys. Rev. C **79**, 034909 (2009).

[128] V. Vovchenko, B. Dönigus, and H. Stoecker, Canonical statistical model analysis of p-p, p-Pb, and Pb-Pb collisions

at energies available at the CERN Large Hadron Collider, Phys. Rev. C **100**, 054906 (2019).
[129] J. Cleymans, P. M. Lo, K. Redlich, and N. Sharma, Multiplicity dependence of (multi)strange baryons in the canonical ensemble with phase shift corrections, Phys. Rev. C **103**, 014904 (2021).
[130] J. Cleymans, H. Oeschler, and K. Redlich, Statistical model description of K^+ and K^- production between 1-10 GeV · A, Phys. Lett. B **485**, 27 (2000).
[131] J. D. Brandenburg, N. Lewis, P. Tribedy, and Z. Xu, Search for baryon junctions in photonuclear processes and isobar collisions at RHIC, arXiv:2205.05685.

S. Acharya,[128] D. Adamová,[87] G. Aglieri Rinella,[33] L. Aglietta,[25] M. Agnello,[30] N. Agrawal,[26] Z. Ahammed,[136] S. Ahmad,[16] S. U. Ahn,[72] I. Ahuja,[38] A. Akindinov,[142] M. Al-Turany,[98] D. Aleksandrov,[142] B. Alessandro,[57] H. M. Alfanda,[6] R. Alfaro Molina,[68] B. Ali,[16] A. Alici,[26] N. Alizadehvandchali,[117] A. Alkin,[33] J. Alme,[21] G. Alocco,[53] T. Alt,[65] A. R. Altamura,[51] I. Altsybeev,[96] J. R. Alvarado,[45] M. N. Anaam,[6] C. Andrei,[46] N. Andreou,[116] A. Andronic,[127] E. Andronov,[142] V. Anguelov,[95] F. Antinori,[55] P. Antonioli,[52] N. Apadula,[75] L. Aphecetche,[104] H. Appelshäuser,[65] C. Arata,[74] S. Arcelli,[26] M. Aresti,[23] R. Arnaldi,[57] J. G. M. C. A. Arneiro,[111] I. C. Arsene,[20] M. Arslandok,[139] A. Augustinus,[33] R. Averbeck,[98] M. D. Azmi,[16] H. Baba,[125] A. Badalà,[54] J. Bae,[105] Y. W. Baek,[41] X. Bai,[121] R. Bailhache,[65] Y. Bailung,[49] R. Bala,[92] A. Balbino,[30] A. Baldisseri,[131] B. Balis,[2] D. Banerjee,[4] Z. Banoo,[92] F. Barile,[32] L. Barioglio,[57] M. Barlou,[79] B. Barman,[42] G. G. Barnaföldi,[47] L. S. Barnby,[86] E. Barreau,[104] V. Barret,[128] L. Barreto,[111] C. Bartels,[120] K. Barth,[33] E. Bartsch,[65] N. Bastid,[128] S. Basu,[76] G. Batigne,[104] D. Battistini,[96] B. Batyunya,[143] D. Bauri,[48] J. L. Bazo Alba,[102] I. G. Bearden,[84] C. Beattie,[139] P. Becht,[98] D. Behera,[49] I. Belikov,[130] A. D. C. Bell Hechavarria,[127] F. Bellini,[26] R. Bellwied,[117] S. Belokurova,[142] L. G. E. Beltran,[110] Y. A. V. Beltran,[45] G. Bencedi,[47] S. Beole,[25] Y. Berdnikov,[142] A. Berdnikova,[95] L. Bergmann,[95] M. G. Besoiu,[64] L. Betev,[33] P. P. Bhaduri,[136] A. Bhasin,[92] M. A. Bhat,[4] B. Bhattacharjee,[42] L. Bianchi,[25] N. Bianchi,[50] J. Bielčík,[36] J. Bielčíková,[87] A. P. Bigot,[130] A. Bilandzic,[96] G. Biro,[47] S. Biswas,[4] N. Bize,[104] J. T. Blair,[109] D. Blau,[142] M. B. Blidaru,[98] N. Bluhme,[39] C. Blume,[65] G. Boca,[22,56] F. Bock,[88] T. Bodova,[21] S. Boi,[23] J. Bok,[17] L. Boldizsár,[47] M. Bombara,[38] P. M. Bond,[33] G. Bonomi,[56,135] H. Borel,[131] A. Borissov,[142] A. G. Borquez Carcamo,[95] H. Bossi,[139] E. Botta,[25] Y. E. M. Bouziani,[65] L. Bratrud,[65] P. Braun-Munzinger,[98] M. Bregant,[111] M. Broz,[36] G. E. Bruno,[32,97] M. D. Buckland,[24] D. Budnikov,[142] H. Buesching,[65] S. Bufalino,[30] P. Buhler,[103] N. Burmasov,[142] Z. Buthelezi,[69,124] A. Bylinkin,[21] S. A. Bysiak,[108] J. C. Cabanillas Noris,[110] M. Cai,[6] H. Caines,[139] A. Caliva,[29] E. Calvo Villar,[102] J. M. M. Camacho,[110] P. Camerini,[24] F. D. M. Canedo,[111] S. L. Cantway,[139] M. Carabas,[114] A. A. Carballo,[33] F. Carnesecchi,[33] R. Caron,[129] L. A. D. Carvalho,[111] J. Castillo Castellanos,[131] F. Catalano,[25,33] S. Cattaruzzi,[24] C. Ceballos Sanchez,[143] R. Cerri,[25] I. Chakaberia,[75] P. Chakraborty,[48] S. Chandra,[136] S. Chapeland,[33] M. Chartier,[120] S. Chattopadhyay,[136] S. Chattopadhyay,[100] T. Cheng,[6,98] C. Cheshkov,[129] V. Chibante Barroso,[33] D. D. Chinellato,[112] E. S. Chizzali,[96,b] J. Cho,[59] S. Cho,[59] P. Chochula,[33] D. Choudhury,[42] P. Christakoglou,[85] C. H. Christensen,[84] P. Christiansen,[76] T. Chujo,[126] M. Ciacco,[30] C. Cicalo,[53] M. R. Ciupek,[98] G. Clai,[52,c] F. Colamaria,[51] J. S. Colburn,[101] D. Colella,[32,97] M. Colocci,[26] M. Concas,[33] G. Conesa Balbastre,[74] Z. Conesa del Valle,[132] G. Contin,[24] J. G. Contreras,[36] M. L. Coquet,[131] P. Cortese,[57,134] M. R. Cosentino,[113] F. Costa,[33] S. Costanza,[22,56] C. Cot,[132] J. Crkovská,[95] P. Crochet,[128] R. Cruz-Torres,[75] P. Cui,[6] A. Dainese,[55] M. C. Danisch,[95] A. Danu,[64] P. Das,[81] P. Das,[4] S. Das,[4] A. R. Dash,[127] S. Dash,[48] A. De Caro,[29] G. de Cataldo,[51] J. de Cuveland,[39] A. De Falco,[23] D. De Gruttola,[29] N. De Marco,[57] C. De Martin,[24] S. De Pasquale,[29] R. Deb,[135] R. Del Grande,[96] L. Dello Stritto,[29,33] W. Deng,[6] P. Dhankher,[19] D. Di Bari,[32] A. Di Mauro,[33] B. Diab,[131] R. A. Diaz,[7,143] T. Dietel,[115] Y. Ding,[6] J. Ditzel,[65] R. Divià,[33] D. U. Dixit,[19] Ø. Djuvsland,[21] U. Dmitrieva,[142] A. Dobrin,[64] B. Dönigus,[65] J. M. Dubinski,[137] A. Dubla,[98] S. Dudi,[91] P. Dupieux,[128] M. Durkac,[107] N. Dzalaiova,[13] T. M. Eder,[127] R. J. Ehlers,[75] F. Eisenhut,[65] R. Ejima,[93] D. Elia,[51] B. Erazmus,[104] F. Ercolessi,[26] B. Espagnon,[132] G. Eulisse,[33] D. Evans,[101] S. Evdokimov,[142] L. Fabbietti,[96] M. Faggin,[28] J. Faivre,[74] F. Fan,[6] W. Fan,[75] A. Fantoni,[50] M. Fasel,[88] A. Feliciello,[57] G. Feofilov,[142] A. Fernández Téllez,[45] L. Ferrandi,[111] M. B. Ferrer,[33] A. Ferrero,[131] C. Ferrero,[57,d] A. Ferretti,[25] V. J. G. Feuillard,[95] V. Filova,[36] D. Finogeev,[142] F. M. Fionda,[53] E. Flatland,[33] F. Flor,[117] A. N. Flores,[109] S. Foertsch,[69] I. Fokin,[95] S. Fokin,[142] E. Fragiacomo,[58] E. Frajna,[47]

U. Fuchs,[33] N. Funicello,[29] C. Furget,[74] A. Furs,[142] T. Fusayasu,[99] J. J. Gaardhøje,[84] M. Gagliardi,[25] A. M. Gago,[102] T. Gahlaut,[48] C. D. Galvan,[110] D. R. Gangadharan,[117] P. Ganoti,[79] C. Garabatos,[98] T. García Chávez,[45] E. Garcia-Solis,[9] C. Gargiulo,[33] P. Gasik,[98] A. Gautam,[119] M. B. Gay Ducati,[67] M. Germain,[104] A. Ghimouz,[126] C. Ghosh,[136] M. Giacalone,[52] G. Gioachin,[30] P. Giubellino,[57,98] P. Giubilato,[28] A. M. C. Glaenzer,[131] P. Glässel,[95] E. Glimos,[123] D. J. Q. Goh,[77] V. Gonzalez,[138] P. Gordeev,[142] M. Gorgon,[2] K. Goswami,[49] S. Gotovac,[34] V. Grabski,[68] L. K. Graczykowski,[137] E. Grecka,[87] A. Grelli,[60] C. Grigoras,[33] V. Grigoriev,[142] S. Grigoryan,[1,143] F. Grosa,[33] J. F. Grosse-Oetringhaus,[33] R. Grosso,[98] D. Grund,[36] N. A. Grunwald,[95] G. G. Guardiano,[112] R. Guernane,[74] M. Guilbaud,[104] K. Gulbrandsen,[84] T. Gündem,[65] T. Gunji,[125] W. Guo,[6] A. Gupta,[92] R. Gupta,[92] R. Gupta,[49] K. Gwizdziel,[137] L. Gyulai,[47] C. Hadjidakis,[132] F. U. Haider,[92] S. Haidlova,[36] M. Haldar,[4] H. Hamagaki,[77] A. Hamdi,[75] Y. Han,[140] B. G. Hanley,[138] R. Hannigan,[109] J. Hansen,[76] J. W. Harris,[139] A. Harton,[9] M. V. Hartung,[65] H. Hassan,[118] D. Hatzifotiadou,[52] P. Hauer,[43] L. B. Havener,[139] E. Hellbär,[98] H. Helstrup,[35] M. Hemmer,[65] T. Herman,[36] G. Herrera Corral,[8] F. Herrmann,[127] S. Herrmann,[129] K. F. Hetland,[35] B. Heybeck,[65] H. Hillemanns,[33] B. Hippolyte,[130] F. W. Hoffmann,[71] B. Hofman,[60] G. H. Hong,[140] M. Horst,[96] A. Horzyk,[2] Y. Hou,[6] P. Hristov,[33] P. Huhn,[65] L. M. Huhta,[118] T. J. Humanic,[89] A. Hutson,[117] D. Hutter,[39] M. C. Hwang,[19] R. Ilkaev,[142] H. Ilyas,[14] M. Inaba,[126] G. M. Innocenti,[33] M. Ippolitov,[142] A. Isakov,[85] T. Isidori,[119] M. S. Islam,[100] M. Ivanov,[98] M. Ivanov,[13] V. Ivanov,[142] K. E. Iversen,[76] M. Jablonski,[2] B. Jacak,[19,75] N. Jacazio,[26] P. M. Jacobs,[75] S. Jadlovska,[107] J. Jadlovsky,[107] S. Jaelani,[83] C. Jahnke,[111] M. J. Jakubowska,[137] M. A. Janik,[137] T. Janson,[71] S. Ji,[17] S. Jia,[10] A. A. P. Jimenez,[66] F. Jonas,[75,88,127] D. M. Jones,[120] J. M. Jowett,[33,98] J. Jung,[65] M. Jung,[65] A. Junique,[33] A. Jusko,[101] J. Kaewjai,[106] P. Kalinak,[61] A. S. Kalteyer,[98] A. Kalweit,[33] A. Karasu Uysal,[73,e] D. Karatovic,[90] O. Karavichev,[142] T. Karavicheva,[142] P. Karczmarczyk,[137] E. Karpechev,[142] M. J. Karwowska,[33,137] U. Kebschull,[71] R. Keidel,[141] D. L. D. Keijdener,[60] M. Keil,[33] B. Ketzer,[43] S. S. Khade,[49] A. M. Khan,[121] S. Khan,[16] A. Khanzadeev,[142] Y. Kharlov,[142] A. Khatun,[119] A. Khuntia,[36] Z. Khuranova,[65] B. Kileng,[35] B. Kim,[105] C. Kim,[17] D. J. Kim,[118] E. J. Kim,[70] J. Kim,[140] J. Kim,[59] J. Kim,[70] M. Kim,[19] S. Kim,[18] T. Kim,[140] K. Kimura,[93] S. Kirsch,[65] I. Kisel,[39] S. Kiselev,[142] A. Kisiel,[137] J. P. Kitowski,[2] J. L. Klay,[5] J. Klein,[33] S. Klein,[75] C. Klein-Bösing,[127] M. Kleiner,[65] T. Klemenz,[96] A. Kluge,[33] C. Kobdaj,[106] T. Kollegger,[98] A. Kondratyev,[143] N. Kondratyeva,[142] J. Konig,[65] S. A. Konigstorfer,[96] P. J. Konopka,[33] G. Kornakov,[137] M. Korwieser,[96] S. D. Koryciak,[2] A. Kotliarov,[87] N. Kovacic,[90] V. Kovalenko,[142] M. Kowalski,[108] V. Kozhuharov,[37] I. Králik,[61] A. Kravčáková,[38] L. Krcal,[33,39] M. Krivda,[61,101] F. Krizek,[87] K. Krizkova Gajdosova,[33] M. Kroesen,[95] M. Krüger,[65] D. M. Krupova,[36] E. Kryshen,[142] V. Kučera,[59] C. Kuhn,[130] P. G. Kuijer,[85] T. Kumaoka,[126] D. Kumar,[136] L. Kumar,[91] N. Kumar,[91] S. Kumar,[32] S. Kundu,[33] P. Kurashvili,[80] A. Kurepin,[142] A. B. Kurepin,[142] A. Kuryakin,[142] S. Kushpil,[87] V. Kuskov,[142] M. Kutyla,[137] M. J. Kweon,[59] Y. Kwon,[140] S. L. La Pointe,[39] P. La Rocca,[27] A. Lakrathok,[106] M. Lamanna,[33] A. R. Landou,[74] R. Langoy,[122] P. Larionov,[33] E. Laudi,[33] L. Lautner,[33,96] R. Lavicka,[103] R. Lea,[56,135] H. Lee,[105] I. Legrand,[46] G. Legras,[127] J. Lehrbach,[39] T. M. Lelek,[2] R. C. Lemmon,[86] I. León Monzón,[110] M. M. Lesch,[96] E. D. Lesser,[19] P. Lévai,[47] X. Li,[10] B. E. Liang-gilman,[19] J. Lien,[122] R. Lietava,[101] I. Likmeta,[117] B. Lim,[25] S. H. Lim,[17] V. Lindenstruth,[39] A. Lindner,[46] C. Lippmann,[98] D. H. Liu,[6] J. Liu,[120] G. S. S. Liveraro,[112] I. M. Lofnes,[21] C. Loizides,[88] S. Lokos,[108] J. Lömker,[60] P. Loncar,[34] X. Lopez,[128] E. López Torres,[7] P. Lu,[98,121] F. V. Lugo,[68] J. R. Luhder,[127] M. Lunardon,[28] G. Luparello,[58] Y. G. Ma,[40] M. Mager,[33] A. Maire,[130] E. M. Majerz,[2] M. V. Makariev,[37] M. Malaev,[142] G. Malfattore,[26] N. M. Malik,[92] Q. W. Malik,[20] S. K. Malik,[92] L. Malinina,[143,a,f] D. Mallick,[132] N. Mallick,[49] G. Mandaglio,[31,54] S. K. Mandal,[80] V. Manko,[142] F. Manso,[128] V. Manzari,[51] Y. Mao,[6] R. W. Marcjan,[2] G. V. Margagliotti,[24] A. Margotti,[52] A. Marín,[98] C. Markert,[109] P. Martinengo,[33] M. I. Martínez,[45] G. Martínez García,[104] M. P. P. Martins,[111] S. Masciocchi,[98] M. Masera,[25] A. Masoni,[53] L. Massacrier,[132] O. Massen,[60] A. Mastroserio,[51,133] O. Matonoha,[76] S. Mattiazzo,[28] A. Matyja,[108] C. Mayer,[108] A. L. Mazuecos,[33] F. Mazzaschi,[25] M. Mazzilli,[33] J. E. Mdhluli,[124] Y. Melikyan,[44] A. Menchaca-Rocha,[68] J. E. M. Mendez,[66] E. Meninno,[103] A. S. Menon,[117] M. Meres,[13] Y. Miake,[126] L. Micheletti,[33] D. L. Mihaylov,[96] K. Mikhaylov,[142,143] D. Miśkowiec,[98] A. Modak,[4] B. Mohanty,[81] M. Mohisin Khan,[16,g] M. A. Molander,[44] S. Monira,[137] C. Mordasini,[118] D. A. Moreira De Godoy,[127] I. Morozov,[142] A. Morsch,[33] T. Mrnjavac,[33] V. Muccifora,[50] S. Muhuri,[136] J. D. Mulligan,[75] A. Mulliri,[23] M. G. Munhoz,[111] R. H. Munzer,[65]

H. Murakami,[125] S. Murray,[115] L. Musa,[33] J. Musinsky,[61] J. W. Myrcha,[137] B. Naik,[124] A. I. Nambrath,[19] B. K. Nandi,[48] R. Nania,[52] E. Nappi,[51] A. F. Nassirpour,[18] A. Nath,[95] C. Nattrass,[123] M. N. Naydenov,[37] A. Neagu,[20] A. Negru,[114] E. Nekrasova,[142] L. Nellen,[66] R. Nepeivoda,[76] S. Nese,[20] G. Neskovic,[39] N. Nicassio,[51] B. S. Nielsen,[84] E. G. Nielsen,[84] S. Nikolaev,[142] S. Nikulin,[142] V. Nikulin,[142] F. Noferini,[52] S. Noh,[12] P. Nomokonov,[143] J. Norman,[120] N. Novitzky,[88] P. Nowakowski,[137] A. Nyanin,[142] J. Nystrand,[21] S. Oh,[18] A. Ohlson,[76] V. A. Okorokov,[142] J. Oleniacz,[137] A. Onnerstad,[118] C. Oppedisano,[57] A. Ortiz Velasquez,[66] J. Otwinowski,[108] M. Oya,[93] K. Oyama,[77] Y. Pachmayer,[95] S. Padhan,[48] D. Pagano,[56,135] G. Paić,[66] S. Paisano-Guzmán,[45] A. Palasciano,[51] S. Panebianco,[131] H. Park,[126] H. Park,[105] J. Park,[59] J. E. Parkkila,[33] Y. Patley,[48] B. Paul,[23] M. M. D. M. Paulino,[111] H. Pei,[6] T. Peitzmann,[60] X. Peng,[11] M. Pennisi,[25] S. Perciballi,[25] D. Peresunko,[142] G. M. Perez,[7] Y. Pestov,[142] V. Petrov,[142] M. Petrovici,[46] R. P. Pezzi,[67,104] S. Piano,[58] M. Pikna,[13] P. Pillot,[104] O. Pinazza,[33,52] L. Pinsky,[117] C. Pinto,[96] S. Pisano,[50] M. Płoskoń,[75] M. Planinic,[90] F. Pliquett,[65] M. G. Poghosyan,[88] B. Polichtchouk,[142] S. Politano,[30] N. Poljak,[90] A. Pop,[46] S. Porteboeuf-Houssais,[128] V. Pozdniakov,[143] I. Y. Pozos,[45] K. K. Pradhan,[49] S. K. Prasad,[4] S. Prasad,[49] R. Preghenella,[52] F. Prino,[57] C. A. Pruneau,[138] I. Pshenichnov,[142] M. Puccio,[33] S. Pucillo,[25] Z. Pugelova,[107] S. Qiu,[85] L. Quaglia,[25] S. Ragoni,[15] A. Rai,[139] A. Rakotozafindrabe,[131] L. Ramello,[57,134] F. Rami,[130] T. A. Rancien,[74] M. Rasa,[27] S. S. Räsänen,[44] R. Rath,[52] M. P. Rauch,[21] I. Ravasenga,[33] K. F. Read,[88,123] C. Reckziegel,[113] A. R. Redelbach,[39] K. Redlich,[80,h] C. A. Reetz,[98] H. D. Regules-Medel,[45] A. Rehman,[21] F. Reidt,[33] H. A. Reme-Ness,[35] Z. Rescakova,[38] K. Reygers,[95] A. Riabov,[142] V. Riabov,[142] R. Ricci,[29] M. Richter,[20] A. A. Riedel,[96] W. Riegler,[33] A. G. Riffero,[25] C. Ristea,[64] M. V. Rodriguez,[33] M. Rodríguez Cahuantzi,[45] S. A. Rodríguez Ramírez,[45] K. Røed,[20] R. Rogalev,[142] E. Rogochaya,[143] T. S. Rogoschinski,[65] D. Rohr,[33] D. Röhrich,[21] P. F. Rojas,[45] S. Rojas Torres,[36] P. S. Rokita,[137] G. Romanenko,[26] F. Ronchetti,[50] A. Rosano,[31,54] E. D. Rosas,[66] K. Roslon,[137] A. Rossi,[55] A. Roy,[49] S. Roy,[48] N. Rubini,[26] D. Ruggiano,[137] R. Rui,[24] P. G. Russek,[2] R. Russo,[85] A. Rustamov,[82] E. Ryabinkin,[142] Y. Ryabov,[142] A. Rybicki,[108] H. Rytkonen,[118] J. Ryu,[17] W. Rzesa,[137] O. A. M. Saarimaki,[44] S. Sadhu,[32] S. Sadovsky,[142] J. Saetre,[21] K. Šafařík,[36] P. Saha,[42] S. K. Saha,[4] S. Saha,[81] B. Sahoo,[49] R. Sahoo,[49] S. Sahoo,[62] D. Sahu,[49] P. K. Sahu,[62] J. Saini,[136] K. Sajdakova,[38] S. Sakai,[126] M. P. Salvan,[98] S. Sambyal,[92] D. Samitz,[103] I. Sanna,[33,96] T. B. Saramela,[111] D. Sarkar,[84] P. Sarma,[42] V. Sarritzu,[23] V. M. Sarti,[96] M. H. P. Sas,[33] S. Sawan,[81] E. Scapparone,[52] J. Schambach,[88] H. S. Scheid,[65] C. Schiaua,[46] R. Schicker,[95] F. Schlepper,[95] A. Schmah,[98] C. Schmidt,[98] H. R. Schmidt,[94] M. O. Schmidt,[33] M. Schmidt,[94] N. V. Schmidt,[88] A. R. Schmier,[123] R. Schotter,[130] A. Schröter,[39] J. Schukraft,[33] K. Schweda,[98] G. Scioli,[26] E. Scomparin,[57] J. E. Seger,[15] Y. Sekiguchi,[125] D. Sekihata,[125] M. Selina,[85] I. Selyuzhenkov,[98] S. Senyukov,[130] J. J. Seo,[95] D. Serebryakov,[142] L. Serkin,[66] L. Šerkšnytė,[96] A. Sevcenco,[64] T. J. Shaba,[69] A. Shabetai,[104] R. Shahoyan,[33] A. Shangaraev,[142] B. Sharma,[92] D. Sharma,[48] H. Sharma,[55] M. Sharma,[92] S. Sharma,[77] S. Sharma,[92] U. Sharma,[92] A. Shatat,[132] O. Sheibani,[117] K. Shigaki,[93] M. Shimomura,[78] J. Shin,[12] S. Shirinkin,[142] Q. Shou,[40] Y. Sibiriak,[142] S. Siddhanta,[53] T. Siemiarczuk,[80] T. F. Silva,[111] D. Silvermyr,[76] T. Simantathammakul,[106] R. Simeonov,[37] B. Singh,[92] B. Singh,[96] K. Singh,[49] R. Singh,[81] R. Singh,[92] R. Singh,[49,98] S. Singh,[16] V. K. Singh,[136] V. Singhal,[136] T. Sinha,[100] B. Sitar,[13] M. Sitta,[57,134] T. B. Skaali,[20] G. Skorodumovs,[95] M. Slupecki,[44] N. Smirnov,[139] R. J. M. Snellings,[60] E. H. Solheim,[20] J. Song,[17] C. Sonnabend,[33,98] J. M. Sonneveld,[85] F. Soramel,[28] A. B. Soto-hernandez,[89] R. Spijkers,[85] I. Sputowska,[108] J. Staa,[76] J. Stachel,[95] I. Stan,[64] P. J. Steffanic,[123] S. F. Stiefelmaier,[95] D. Stocco,[104] I. Storehaug,[20] P. Stratmann,[127] S. Strazzi,[26] A. Sturniolo,[31,54] C. P. Stylianidis,[85] A. A. P. Suaide,[111] C. Suire,[132] M. Sukhanov,[142] M. Suljic,[33] R. Sultanov,[142] V. Sumberia,[92] S. Sumowidagdo,[83] I. Szarka,[13] M. Szymkowski,[137] S. F. Taghavi,[96] G. Taillepied,[98] J. Takahashi,[112] G. J. Tambave,[81] S. Tang,[6] Z. Tang,[121] J. D. Tapia Takaki,[119] N. Tapus,[114] L. A. Tarasovicova,[127] M. G. Tarzila,[46] G. F. Tassielli,[32] A. Tauro,[33] A. Tavira García,[132] G. Tejeda Muñoz,[45] A. Telesca,[33] L. Terlizzi,[25] C. Terrevoli,[117] S. Thakur,[4] D. Thomas,[109] A. Tikhonov,[142] N. Tiltmann,[33,127] A. R. Timmins,[117] M. Tkacik,[107] T. Tkacik,[107] A. Toia,[65] R. Tokumoto,[93] K. Tomohiro,[93] N. Topilskaya,[142] M. Toppi,[50] T. Tork,[132] V. V. Torres,[104] A. G. Torres Ramos,[32] A. Trifiró,[31,54] A. S. Triolo,[31,33,54] S. Tripathy,[52] T. Tripathy,[48] S. Trogolo,[33] V. Trubnikov,[3] W. H. Trzaska,[118] T. P. Trzcinski,[137] A. Tumkin,[142] R. Turrisi,[55] T. S. Tveter,[20] K. Ullaland,[21] B. Ulukutlu,[96] A. Uras,[129] M. Urioni,[135] G. L. Usai,[23] M. Vala,[38] N. Valle,[22] L. V. R. van Doremalen,[60] M. van Leeuwen,[85] C. A. van Veen,[95]

R. J. G. van Weelden,[85] P. Vande Vyvre,[33] D. Varga,[47] Z. Varga,[47] P. Vargas Torres,[66] M. Vasileiou,[79] A. Vasiliev,[142] O. Vázquez Doce,[50] O. Vazquez Rueda,[117] V. Vechernin,[142] E. Vercellin,[25] S. Vergara Limón,[45] R. Verma,[48] L. Vermunt,[98] R. Vértesi,[47] M. Verweij,[60] L. Vickovic,[34] Z. Vilakazi,[124] O. Villalobos Baillie,[101] A. Villani,[24] A. Vinogradov,[142] T. Virgili,[29] M. M. O. Virta,[118] V. Vislavicius,[76] A. Vodopyanov,[143] B. Volkel,[33] M. A. Völkl,[95] S. A. Voloshin,[138] G. Volpe,[32] B. von Haller,[33] I. Vorobyev,[33] N. Vozniuk,[142] J. Vrláková,[38] J. Wan,[40] C. Wang,[40] D. Wang,[40] Y. Wang,[40] Y. Wang,[6] A. Wegrzynek,[33] F. T. Weiglhofer,[39] S. C. Wenzel,[33] J. P. Wessels,[127] J. Wiechula,[65] J. Wikne,[20] G. Wilk,[80] J. Wilkinson,[98] G. A. Willems,[127] B. Windelband,[95] M. Winn,[131] J. R. Wright,[109] W. Wu,[40] Y. Wu,[121] Z. Xiong,[121] R. Xu,[6] A. Yadav,[43] A. K. Yadav,[136] S. Yalcin,[73] Y. Yamaguchi,[93] S. Yang,[21] S. Yano,[93] E. R. Yeats,[19] Z. Yin,[6] I.-K. Yoo,[17] J. H. Yoon,[59] H. Yu,[12] S. Yuan,[21] A. Yuncu,[95] V. Zaccolo,[24] C. Zampolli,[33] F. Zanone,[95] N. Zardoshti,[33] A. Zarochentsev,[142] P. Závada,[63] N. Zaviyalov,[142] M. Zhalov,[142] B. Zhang,[6] C. Zhang,[131] L. Zhang,[40] M. Zhang,[6] S. Zhang,[40] X. Zhang,[6] Y. Zhang,[121] Z. Zhang,[6] M. Zhao,[10] V. Zherebchevskii,[142] Y. Zhi,[10] C. Zhong,[40] D. Zhou,[6] Y. Zhou,[84] J. Zhu,[6,55] Y. Zhu,[6] S. C. Zugravel,[57] and N. Zurlo[56,135]

(ALICE Collaboration)

[1]*A.I. Alikhanyan National Science Laboratory (Yerevan Physics Institute) Foundation, Yerevan, Armenia*
[2]*AGH University of Krakow, Cracow, Poland*
[3]*Bogolyubov Institute for Theoretical Physics, National Academy of Sciences of Ukraine, Kiev, Ukraine*
[4]*Bose Institute, Department of Physics and Centre for Astroparticle Physics and Space Science (CAPSS), Kolkata, India*
[5]*California Polytechnic State University, California, USA*
[6]*Central China Normal University, Wuhan, China*
[7]*Centro de Aplicaciones Tecnológicas y Desarrollo Nuclear (CEADEN), Havana, Cuba*
[8]*Centro de Investigación y de Estudios Avanzados (CINVESTAV), Mexico City and Mérida, Mexico*
[9]*Chicago State University, Chicago, Illinois, USA*
[10]*China Institute of Atomic Energy, Beijing, China*
[11]*China University of Geosciences, Wuhan, China*
[12]*Chungbuk National University, Cheongju, Republic of Korea*
[13]*Comenius University Bratislava, Faculty of Mathematics, Physics and Informatics, Bratislava, Slovak Republic*
[14]*COMSATS University Islamabad, Bratislava, Slovak Republic*
[15]*Creighton University, Omaha, Nebraska, USA*
[16]*Department of Physics, Aligarh Muslim University, Aligarh, India*
[17]*Department of Physics, Pusan National University, Pusan, Republic of Korea*
[18]*Department of Physics, Sejong University, Seoul, Republic of Korea*
[19]*Department of Physics, University of California, Berkeley, California, USA*
[20]*Department of Physics, University of Oslo, Oslo, Norway*
[21]*Department of Physics and Technology, University of Bergen, Bergen, Norway*
[22]*Dipartimento di Fisica, Università di Pavia, Pavia, Italy*
[23]*Dipartimento di Fisica dell'Università and Sezione INFN, Cagliari, Italy*
[24]*Dipartimento di Fisica dell'Università and Sezione INFN, Trieste, Italy*
[25]*Dipartimento di Fisica dell'Università and Sezione INFN, Turin, Italy*
[26]*Dipartimento di Fisica e Astronomia dell'Università and Sezione INFN, Bologna, Italy*
[27]*Dipartimento di Fisica e Astronomia dell'Università and Sezione INFN, Catania, Italy*
[28]*Dipartimento di Fisica e Astronomia dell'Università and Sezione INFN, Padova, Italy*
[29]*Dipartimento di Fisica 'E.R. Caianiello' dell'Università and Gruppo Collegato INFN, Salerno, Italy*
[30]*Dipartimento DISAT del Politecnico and Sezione INFN, Turin, Italy*
[31]*Dipartimento di Scienze MIFT, Università di Messina, Messina, Italy*
[32]*Dipartimento Interateneo di Fisica 'M. Merlin' and Sezione INFN, Bari, Italy*
[33]*European Organization for Nuclear Research (CERN), Geneva, Switzerland*
[34]*Faculty of Electrical Engineering, Mechanical Engineering and Naval Architecture, University of Split, Split, Croatia*
[35]*Faculty of Engineering and Science, Western Norway University of Applied Sciences, Bergen, Norway*
[36]*Faculty of Nuclear Sciences and Physical Engineering, Czech Technical University in Prague, Prague, Czech Republic*
[37]*Faculty of Physics, Sofia University, Sofia, Bulgaria*
[38]*Faculty of Science, P.J. Šafárik University, Košice, Slovak Republic*
[39]*Frankfurt Institute for Advanced Studies, Johann Wolfgang Goethe-Universität Frankfurt, Frankfurt, Germany*
[40]*Fudan University, Shanghai, China*

[41]Gangneung-Wonju National University, Gangneung, Republic of Korea
[42]Gauhati University, Department of Physics, Guwahati, India
[43]Helmholtz-Institut für Strahlen- und Kernphysik, Rheinische Friedrich-Wilhelms-Universität Bonn, Bonn, Germany
[44]Helsinki Institute of Physics (HIP), Helsinki, Finland
[45]High Energy Physics Group, Universidad Autónoma de Puebla, Puebla, Mexico
[46]Horia Hulubei National Institute of Physics and Nuclear Engineering, Bucharest, Romania
[47]HUN-REN Wigner Research Centre for Physics, Budapest, Hungary
[48]Indian Institute of Technology Bombay (IIT), Mumbai, India
[49]Indian Institute of Technology Indore, Indore, India
[50]INFN, Laboratori Nazionali di Frascati, Frascati, Italy
[51]INFN, Sezione di Bari, Bari, Italy
[52]INFN, Sezione di Bologna, Bologna, Italy
[53]INFN, Sezione di Cagliari, Cagliari, Italy
[54]INFN, Sezione di Catania, Catania, Italy
[55]INFN, Sezione di Padova, Padova, Italy
[56]INFN, Sezione di Pavia, Pavia, Italy
[57]INFN, Sezione di Torino, Turin, Italy
[58]INFN, Sezione di Trieste, Trieste, Italy
[59]Inha University, Incheon, Republic of Korea
[60]Institute for Gravitational and Subatomic Physics (GRASP), Utrecht University/Nikhef, Utrecht, Netherlands
[61]Institute of Experimental Physics, Slovak Academy of Sciences, Košice, Slovak Republic
[62]Institute of Physics, Homi Bhabha National Institute, Bhubaneswar, India
[63]Institute of Physics of the Czech Academy of Sciences, Prague, Czech Republic
[64]Institute of Space Science (ISS), Bucharest, Romania
[65]Institut für Kernphysik, Johann Wolfgang Goethe-Universität Frankfurt, Frankfurt, Germany
[66]Instituto de Ciencias Nucleares, Universidad Nacional Autónoma de México, Mexico City, Mexico
[67]Instituto de Física, Universidade Federal do Rio Grande do Sul (UFRGS), Porto Alegre, Brazil
[68]Instituto de Física, Universidad Nacional Autónoma de México, Mexico City, Mexico
[69]iThemba LABS, National Research Foundation, Somerset West, South Africa
[70]Jeonbuk National University, Jeonju, Republic of Korea
[71]Johann-Wolfgang-Goethe Universität Frankfurt Institut für Informatik, Fachbereich Informatik und Mathematik, Frankfurt, Germany
[72]Korea Institute of Science and Technology Information, Daejeon, Republic of Korea
[73]KTO Karatay University, Konya, Turkey
[74]Laboratoire de Physique Subatomique et de Cosmologie, Université Grenoble-Alpes, CNRS-IN2P3, Grenoble, France
[75]Lawrence Berkeley National Laboratory, Berkeley, California, USA
[76]Lund University Department of Physics, Division of Particle Physics, Lund, Sweden
[77]Nagasaki Institute of Applied Science, Nagasaki, Japan
[78]Nara Women's University (NWU), Nara, Japan
[79]National and Kapodistrian University of Athens, School of Science, Department of Physics, Athens, Greece
[80]National Centre for Nuclear Research, Warsaw, Poland
[81]National Institute of Science Education and Research, Homi Bhabha National Institute, Jatni, India
[82]National Nuclear Research Center, Baku, Azerbaijan
[83]National Research and Innovation Agency - BRIN, Jakarta, Indonesia
[84]Niels Bohr Institute, University of Copenhagen, Copenhagen, Denmark
[85]Nikhef, National institute for subatomic physics, Amsterdam, Netherlands
[86]Nuclear Physics Group, STFC Daresbury Laboratory, Daresbury, United Kingdom
[87]Nuclear Physics Institute of the Czech Academy of Sciences, Husinec-Řež, Czech Republic
[88]Oak Ridge National Laboratory, Oak Ridge, Tennessee, USA
[89]Ohio State University, Columbus, Ohio, USA
[90]Physics department, Faculty of science, University of Zagreb, Zagreb, Croatia
[91]Physics Department, Panjab University, Chandigarh, India
[92]Physics Department, University of Jammu, Jammu, India
[93]Physics Program and International Institute for Sustainability with Knotted Chiral Meta Matter (SKCM2), Hiroshima University, Hiroshima, Japan
[94]Physikalisches Institut, Eberhard-Karls-Universität Tübingen, Tubingen, Germany
[95]Physikalisches Institut, Ruprecht-Karls-Universität Heidelberg, Heidelberg, Germany
[96]Physik Department, Technische Universität München, Munich, Germany
[97]Politecnico di Bari and Sezione INFN, Bari, Italy

[98]Research Division and ExtreMe Matter Institute EMMI, GSI Helmholtzzentrum für Schwerionenforschung GmbH, Darmstadt, Germany
[99]Saga University, Saga, Japan
[100]Saha Institute of Nuclear Physics, Homi Bhabha National Institute, Kolkata, India
[101]School of Physics and Astronomy, University of Birmingham, Birmingham, United Kingdom
[102]Sección Física, Departamento de Ciencias, Pontificia Universidad Católica del Perú, Lima, Peru
[103]Stefan Meyer Institut für Subatomare Physik (SMI), Vienna, Austria
[104]SUBATECH, IMT Atlantique, Nantes Université, CNRS-IN2P3, Nantes, France
[105]Sungkyunkwan University, Suwon City, Republic of Korea
[106]Suranaree University of Technology, Nakhon Ratchasima, Thailand
[107]Technical University of Košice, Košice, Slovak Republic
[108]The Henryk Niewodniczanski Institute of Nuclear Physics, Polish Academy of Sciences, Cracow, Poland
[109]The University of Texas at Austin, Austin, Texas, USA
[110]Universidad Autónoma de Sinaloa, Culiacán, Mexico
[111]Universidade de São Paulo (USP), São Paulo, Brazil
[112]Universidade Estadual de Campinas (UNICAMP), Campinas, Brazil
[113]Universidade Federal do ABC, Santo Andre, Brazil
[114]Universitatea Nationala de Stiinta si Tehnologie Politehnica Bucuresti, Bucharest, Romania
[115]University of Cape Town, Cape Town, South Africa
[116]University of Derby, Derby, United Kingdom
[117]University of Houston, Houston, Texas, USA
[118]University of Jyväskylä, Jyvaskyla, Finland
[119]University of Kansas, Lawrence, Kansas, USA
[120]University of Liverpool, Liverpool, United Kingdom
[121]University of Science and Technology of China, Hefei, China
[122]University of South-Eastern Norway, Kongsberg, Norway
[123]University of Tennessee, Knoxville, Tennessee, USA
[124]University of the Witwatersrand, Johannesburg, South Africa
[125]University of Tokyo, Tokyo, Japan
[126]University of Tsukuba, Tsukuba, Japan
[127]Universität Münster, Institut für Kernphysik, Munster, Germany
[128]Université Clermont Auvergne, CNRS/IN2P3, LPC, Clermont-Ferrand, France
[129]Université de Lyon, CNRS/IN2P3, Institut de Physique des 2 Infinis de Lyon, Lyon, France
[130]Université de Strasbourg, CNRS, IPHC UMR 7178, F-67000 Strasbourg, France, Strasbourg, France
[131]Université Paris-Saclay, Centre d'Etudes de Saclay (CEA), IRFU, Départment de Physique Nucléaire (DPhN), Saclay, France
[132]Université Paris-Saclay, CNRS/IN2P3, IJCLab, Orsay, France
[133]Università degli Studi di Foggia, Foggia, Italy
[134]Università del Piemonte Orientale, Vercelli, Italy
[135]Università di Brescia, Brescia, Italy
[136]Variable Energy Cyclotron Centre, Homi Bhabha National Institute, Kolkata, India
[137]Warsaw University of Technology, Warsaw, Poland
[138]Wayne State University, Detroit, Michigan, USA
[139]Yale University, New Haven, Connecticut, USA
[140]Yonsei University, Seoul, Republic of Korea
[141]Zentrum für Technologie und Transfer (ZTT), Worms, Germany
[142]Affiliated with an institute covered by a cooperation agreement with CERN
[143]Affiliated with an international laboratory covered by a cooperation agreement with CERN

[a]Deceased.
[b]Also at Max-Planck-Institut fur Physik, Munich, Germany.
[c]Also at Italian National Agency for New Technologies, Energy and Sustainable Economic Development (ENEA), Bologna, Italy.
[d]Also at Dipartimento DET del Politecnico di Torino, Turin, Italy.
[e]Also at Yildiz Technical University, Istanbul, Türkiye.
[f]Also at An institution covered by a cooperation agreement with CERN.
[g]Also at Department of Applied Physics, Aligarh Muslim University, Aligarh, India.
[h]Also at Institute of Theoretical Physics, University of Wroclaw, Poland.